CANADA

DEPARTMENT OF
ENERGY, MINES AND RESOURCES
MINES BRANCH
OTTAWA

THE DETERMINATION OF MASS ATTENUATION COEFFICIENTS FOR TITANIUM, VANADIUM, IRON, NICKEL, COPPER, PRASEODYMIUM, GADOLINIUM, AND ERBIUM

J. L. DALTON

MINERAL SCIENCES DIVISION

NOVEMBER 1969

Research Report R 211

Price 75 cents

Available by mail from the Queen's Printer, Ottawa
and at the following Canadian Government bookshops

HALIFAX
1735 Barrington Street

MONTREAL
Æterna-Vie Building, 1182 St. Catherine St. West

OTTAWA
Daly Building, Corner Mackenzie and Rideau

TORONTO
221 Yonge Street

WINNIPEG
Mall Center Bldg., 499 Portage Avenue

VANCOUVER
657 Granville Street

or through your bookseller

Price 75 cents Catalogue No. M38-1/211

Price subject to change without notice

Queen's Printer for Canada
Ottawa, 1970

Mines Branch Research Report R 211

THE DETERMINATION OF MASS ATTENUATION COEFFICIENTS FOR TITANIUM, VANADIUM, IRON, NICKEL, COPPER, PRASEODYMIUM, GADOLINIUM, AND ERBIUM

by

J. L. Dalton*

- - -

ABSTRACT

Mass attenuation coefficients have been determined for titanium, vanadium, iron, nickel, copper, praseodymium, gadolinium, and erbium. The coefficients for the transition elements were measured over the range 17 keV to 2 keV and the rare earth elements over the range 28 keV to 5 keV. The precision of the measurements -- that is, the calculated relative sample standard deviation for all the replications for a single coefficient -- was less than one per cent in some cases. Agreement of the standard deviation predicted by the law of propagation of error with that obtained by measurement was achieved in favourable cases. Absorbing foils that were not ideally uniform accounted for discrepancies between the predicted and the actual standard deviations that occurred. The accuracy of the measurements is judged to be in the range two to four per cent of the mass attenuation coefficient reported. A statistical analysis of the data yielded constants and exponents making possible the calculation of mass attenuation coefficients in several atomic number-energy regions.

---

*Scientific Officer, Spectrochemistry Section, Mineral Sciences Division, Mines Branch, Department of Energy, Mines and Resources, Ottawa, Canada.

Direction des mines

Rapport de recherches R 211

DÉTERMINATION DU COEFFICIENT D'ATTÉNUATION DE LA MASSE DU TITANE, DU VANADIUM, DU FER, DU NICKEL, DU CUIVRE, DU PRASÉODYME, DU GADOLINIUM ET DE L'ERBIUM

par

J. L. Dalton*

- - - - - - -

RÉSUMÉ

Le coefficient d'atténuation de la masse du titane, du vanadium, du fer, du nickel, du cuivre, du praséodyme, du gadolinium et de l'erbium a été déterminé. Le coefficient des éléments de transition a été mesuré sous une tension de 17 keV à 2 keV et celui des terres rares sous une tension de 28 keV à 5 keV. Le degré de précision des mesures, c'est à dire l'écart-type relatif de l'échantillon pour toutes les répétitions relativement à un seul coefficient, était de moins d'un p. 100 dans certains cas. La concordance de l'écart-type établie par la loi de la propagation de l'erreur avec l'écart mesuré a été réussie dans certains cas idéals. Les divergences qui se sont révélées entre les écarts-types prévus et ceux qui se sont produits étaient dues au manque d'uniformité de la feuille d'absorption. Les mesures ont été jugées exactes jusqu'à deux à quatre p. 100 du coefficient d'atténuation de la masse rapporté. L'analyse statistique des données obtenues a livré des exposants et des constantes qui ont permis de calculer le coefficient d'atténuation de la masse dans plusieurs zones de la corrélation nombre atomique-énergie.

---

*Agent scientifique, Section de la spectrochimie, Division des sciences minérales, Direction des mines, ministère de l'Énergie, des Mines et des Ressources, Ottawa, Canada.

CONTENTS

= = =

FIGURES

TABLES

- cont'd

TABLES (Continued)

= = =

INTRODUCTION

When a beam of X-rays of intensity I passes through matter of thickness x, experiments have shown, the decrease in intensity of the incident beam is given by the exponential expression:

$$\frac{dI}{I} = -\mu\, dx \qquad \ldots (1)$$

where μ is the linear absorption coefficient and is dependent on the absorber, the density of the absorber, and the energy of the X-rays. Integration of Equation 1 gives:

$$I = I_o \exp(-\mu x) \qquad \ldots (2)$$

where I is the intensity of the transmitted beam. The linear absorption coefficient is proportional to the density ρ and therefore the quantity μ/ρ is a constant of the material and independent of its physical state. The mass absorption coefficient is thus defined as the linear absorption coefficient divided by the density of the material and is the coefficient most frequently tabulated. Equation 2 is then rewritten in a more convenient form as:

$$I = I_o \exp\left(-\frac{\mu}{\rho}\ \rho x\right) \qquad \ldots (3)$$

Several communications (1, 2, 3, 4, 5, 6) have appeared in the recent scientific literature, deploring the lack of accurate mass attenuation coefficients. One would think that such simple material constants would be well known, but the present situation has arisen because of a decline of interest in this area of X-ray physics. Thus, constants that were determined by relatively primitive methods on impure materials have come into use. Further, some of the early workers did not distinguish between coefficients determined by experiment and coefficients determined by extrapolation, thus compounding an undesirable situation.

There have been several published compilations of mass attenuation coefficients in the past. The obsolete but time-honoured compilation due to S.J.M. Allen appeared in Compton and Allison's book (7) in 1935. Allen used his own measurements, in conjunction with published data, in a weighting and extrapolation method to compile the data. In 1963, Stainer published a literature survey (3) of the experimental determination of mass attenuation coefficients. Stainer's survey is notable in that attempts to include the accuracy of the experimental determinations were made. These two compilations were among the foremost in the literature, prior to Heinrich's (2) calculations.

The bar graph in Figure 1 was tabulated by Heinrich (2) at the National Bureau of Standards in Washington. He examined all the published data on mass attenuation coefficients for self consistency and proper technique and then used selected data as a basis for interpolation according to the method of Leroux (5). Leroux proposed a self-consistent set of mass absorption coefficients, using the exponential expression:

$$\mu/\rho = C\lambda^n \qquad \ldots (4)$$

where λ is the wavelength in angstroms (A), μ/p the coefficient, and C and n are determined empirically. The values of C are assumed to vary in a regular fashion as a function of the atomic number of the absorber. From the values of C and n obtained by the analysis of the selected data, Heinrich calculated the mass attenuation coefficients of most of the elements for the K_α, K_β, L_α, L_β, M_α, and M_β lines of many elements. Heinrich's tables are believed to be more reliable than previous sources but it must be borne in mind that his tables have been derived from the data illustrated in Figure 1.

Mass attenuation coefficients are used throughout the field of X-ray technology. In X-ray diffraction, they appear in the exact expression for the intensity diffracted by a single-phase powder specimen and in the equation for the intensity ratio of a two-phase mixture. In electron probe microanalysis, the absorption correction that is applied to the measured

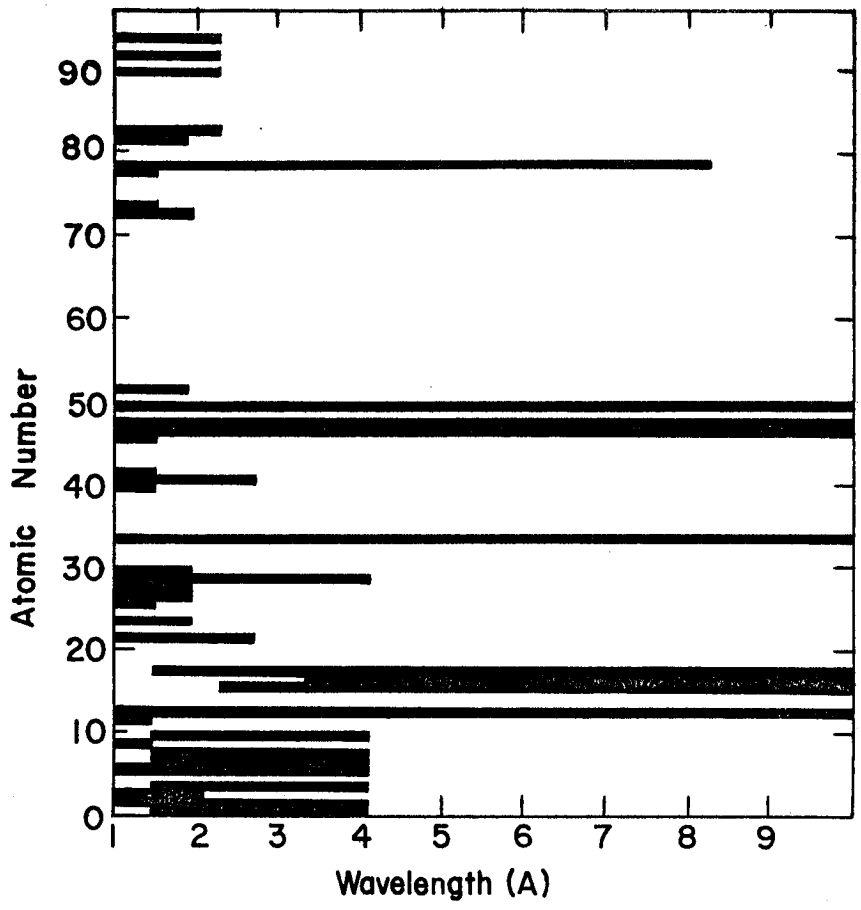

Figure 1. Regions in which mass attenuation coefficients have been experimentally determined (1966).

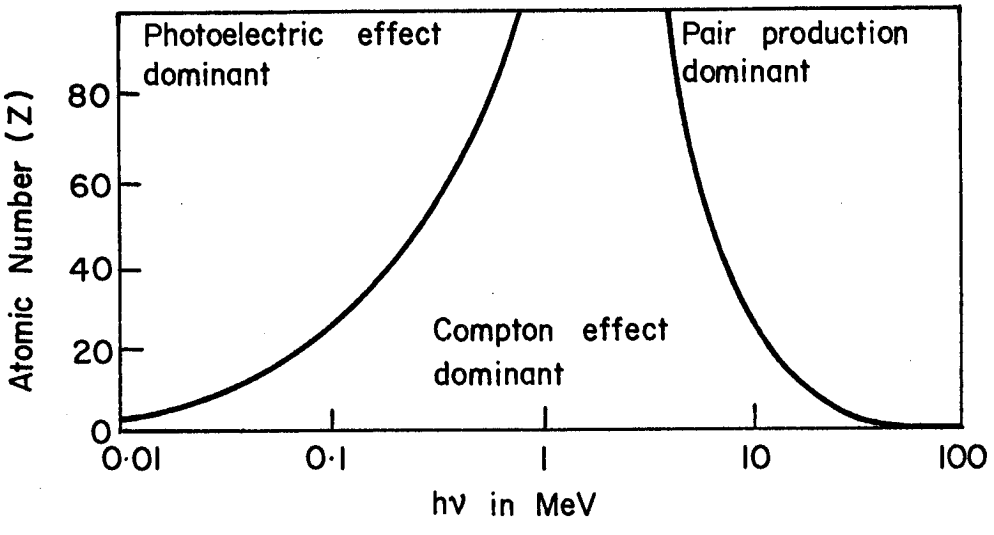

Figure 2. Locus of equal atomic cross-sections for Compton and photoelectric interactions and for Compton and pair-production interactions. The incident photon energy is hν and Z is the atomic number of the absorber.

intensity is large, and the accuracy of this correction varies directly as the accuracy of the mass attenuation coefficient. In X-ray fluorescence spectrometry, the coefficients are used in the calculations relating composition and observed intensity. These calculations are carried out over a wide wavelength range for all the elements present in the specimen undergoing analysis.

The purpose of the present study was to expand the experimental knowledge of mass attenuation coefficients in the energy range 28 keV to 2 keV (λ = 0.5 A to λ = 5A). The choice of absorbing elements for this study was titanium, vanadium, iron, nickel, copper, praseodymium, gadolinium, and erbium. As can be seen from Figure 1, coefficients for some of these elements had previously been measured over the pertinent energy range, but it was advantageous to have some overlap of data.

There are many possible types of interaction between electromagnetic radiation and atoms, electrons and nuclei. The three predominant phenomena are the photoelectric effect, elastic and inelastic scattering, and pair production. The relative importance of these varies with the energy of the incident photon and with the atomic number of the absorbing material. This is illustrated in Figure 2 (8). The phenomenon of pair production will not be discussed, because it is beyond the energy range of this discussion.

The most important attenuation process at photon energies up to 500 keV is the photoelectric effect, defined as the absorption of a photon with subsequent ejection of an electron from the atom. The energy of the ejected atomic electron is equal to the energy of the incident photon minus the binding energy of the atomic electron. For incident energies greater than the K-edge energy, electrons in the K and L shells account for most of the attenuation by this process.

Photons with energy much in excess of that required to eject an electron are unlikely to be absorbed, and therefore photoelectric absorption decreases rapidly as the photon energy increases. At low energies the photoelectric effect varies as $E^{-7/2}$; at high energies, as E^{-1}; where

E is the energy of the incident photon. In addition, the probability of the photoelectric effect occurring exhibits a rapid increase as the atomic number of the absorbing material increases, varying approximately as Z^5.

Coherent or elastic scattering occurs when the photon is deflected without loss of energy. The atom as a whole absorbs the momentum change, and the scattered photon has the same energy as the incident radiation. The photoelectric effect is nevertheless the dominant absorption mechanism in the energy region where coherent scattering occurs.

In the case of incoherent scattering, the atomic electron absorbs some of the momentum from the interaction and either remains in an excited state or leaves the atom, and the scattered photon has less energy than the incident. The theory of incoherent scattering is most satisfactory for photon energies so large, in comparison with electron binding energies, that the electrons can be considered as free. Incoherent scattering by free electrons is known as the Compton effect, and its magnitude is described by the theoretical Klein-Nishina cross-section (9).

G. White Grodstein (10) and, more recently, J. H. Hubbell (11) have calculated attenuation coefficients for a number of elements and compounds over the energy range 10 keV to 100 GeV. Grodstein based her calculations on a number of theoretical derivations and found it necessary to use three of these plus graphical adjustment to calculate the photoelectric cross-section. The uncertainty in the calculated photoelectric cross-section was estimated to be five to fifteen per cent. The error in the total attenuation coefficient was judged to approach ten per cent below 50 keV. Hubbell relied on high-precision total attenuation coefficient measurement in the range 10 keV to 0.2 MeV to calculate the photoelectric cross-section. Grodstein's and Hubbell's compilations emphasize the contribution the various absorption phenomena make to the total attenuation coefficient and thus are intended for those engaged in high-energy radiation research rather than for the X-ray spectroscopist dealing with low energies.

EXPERIMENTAL ASPECTS

The determination of X-ray mass attenuation coefficients consists of measuring the intensity of a collimated monochromatic beam of X-rays under two conditions, one with an absorbing foil in the X-ray path and the other with the path vacant. The absorbing foil should be a single element in a state of high purity and of uniform thickness. Further, since the weight and area of the foil are used to calculate the coefficient, the shape of the foil must be such that the area may be accurately measured.

A Norelco 100-kV constant-potential single-crystal spectrometer was used for the X-ray measurements, and a schematic diagram of this spectrometer is given in Figure 3. The Soller collimators, located before and after the analyzing crystal, were used to collimate the beam. The spacing of the first collimators is 0.005 inch and 0.020 inch for use with medium and long wavelengths respectively, and the spacing for the second collimator is 0.020 inch. Three analyzing crystals, listed in Table 1, were available. The spectrometer is equipped with two detectors in tandem, a gas-flow proportional counter leading and a scintillation counter trailing.

It was necessary to design and construct a device to insert the absorbing foil into the X-ray path. A preliminary investigation with temporary foil holders located before and after the analyzing crystal was carried out. The results are given in Table 2. It was concluded from these results that the coefficient was independent of position in the X-ray path. Accordingly, the device was designed to fit into the most convenient position in the spectroscopy chamber, that is, between the crystal and the first collimator. The device may be described simply as a rotating brass disc, 6 3/4 inches in diameter, wherein four ports were cut. Three of the four ports are used for absorbers and one remains empty for incident intensity measurement. Photographs of the device are reproduced in Figure 4.

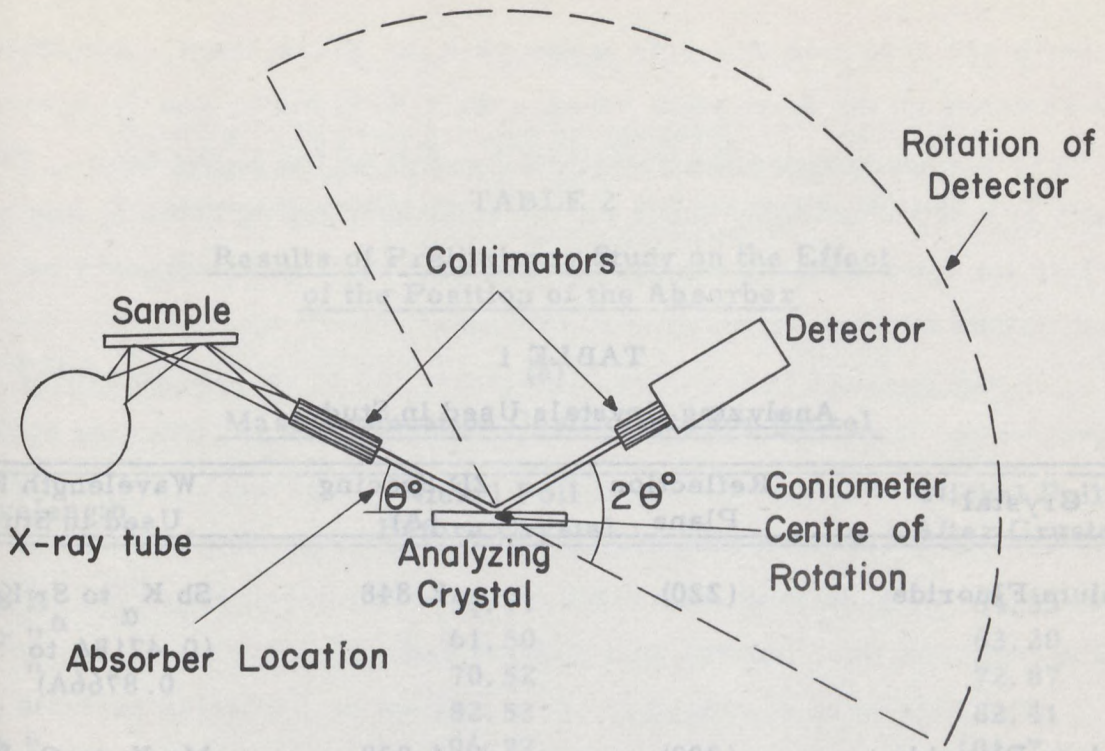

Figure 3. Basic geometry of the Norelco 100kv constant-potential, single-crystal spectrometer.

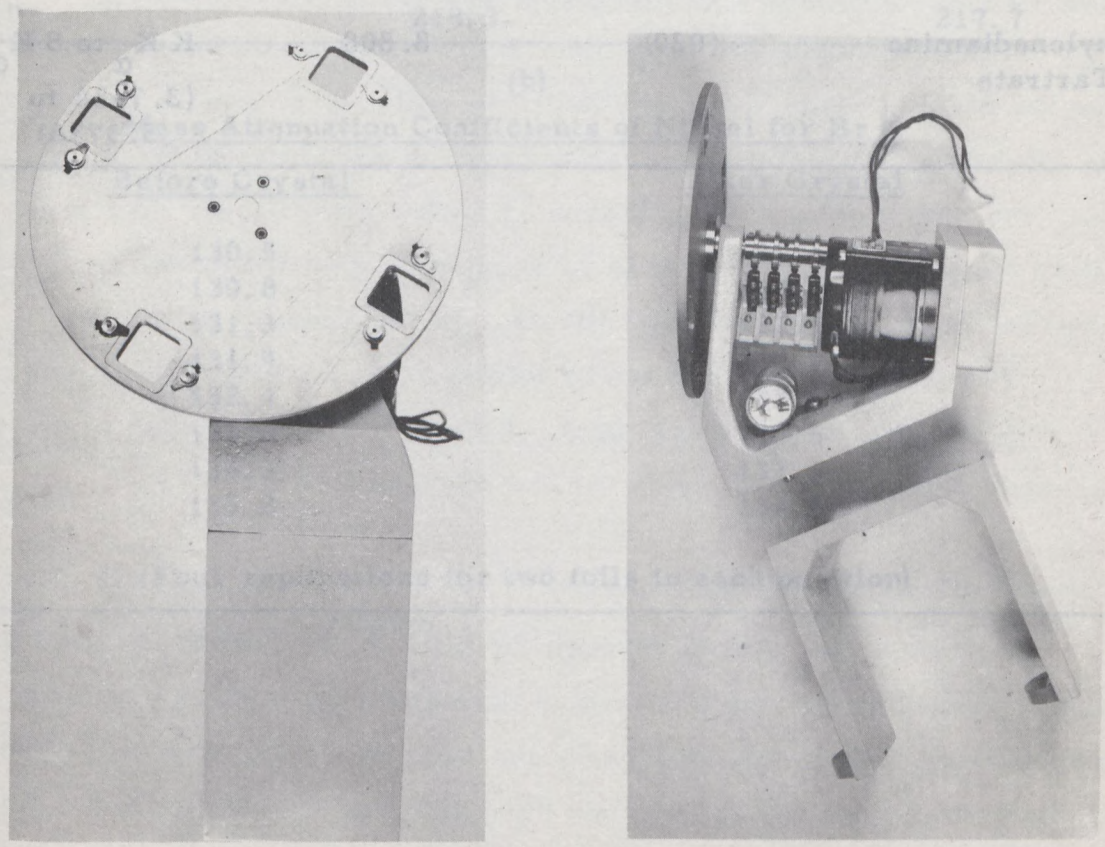

(a) Front view (b) Side view

Figure 4. Photographs of device constructed to insert absorbers into the X-ray path.

TABLE 1

Analyzing Crystals Used in Study

Crystal	Reflection Plane	2D Spacing (A)	Wavelength Range Used in Study
Lithium Fluoride	(220)	2.848	Sb K_α to Sr K_α (0.4718A to 0.8766A)
Lithium Fluoride	(200)	4.028	Mo K_α to Ca K_α (0.7107A to 3.359A)
Ethylenediamine Tartrate	(020)	8.808	K K_α to S K_α (3.742A to 5.373A)

TABLE 2

Results of Preliminary Study on the Effect of the Position of the Absorber

(a)

Mass Attenuation Coefficients for Nickel

Wavelength	Nickel Foil Before Crystal	Nickel Foil After Crystal
Nb K	53.71	54.33
Zr " α	61.50	63.20
Y "	70.52	72.87
Sr "	82.53	82.41
Rb "	96.22	101.7
Br "	131.3	131.6
Se "	157.1	157.3
As "	185.4	184.4
Ge "	218.3	217.7

(b)

Mass Attenuation Coefficients of Nickel for Br K

Before Crystal	After Crystal
130.5	131.6
130.8	132.0
131.3	132.1
131.9	132.7
132.4	133.4
133.6	133.5
134.3	133.5
135.2	134.8

(Four replications for two folls in each position)

The ports are 1/16 inch on a side larger than the X-ray beam. Adjustable limit switches on the drive shaft between the 1-RPM motor and the brass disc were used to position the ports with respect to the X-ray beam. The results of a reproducibility check on the rotating disc, in Table 3, show that both the spectrometer and the rotating disc device are adequate for measurement of mass attenuation coefficients.

It was possible to purchase high-purity foil at various thickness ranges for the elements studied. Copper, nickel, iron and titanium at the 20-micron range and vanadium at the 40-micron range were purchased from Materials Research Corporation, of Orangeburg, New York. Praseodymium, gadolinium and erbium at the 40-micron range were purchased from Johnson, Matthey and Mallory Ltd.

The foils were examined for purity by optical emission analysis and X-ray fluorescence analysis. Praseodymium was analyzed by wet chemical methods for the praseodymium content, to ascertain the extent of oxidation. The results of these analyses are given in Table 4.

The attenuation of the incident X-ray beam would be extremely large over the entire energy range studied if the foils were used as received. It was therefore desirable to use some means of reducing the thickness of the foils, and "pack-rolling" was chosen as such a means (12). In a pack-rolling operation, the material to be reduced is placed between two sheets of thicker metal and rolled until the desired thickness is attained.

The pack was constructed by folding in half a 2-inch by 6-inch piece of 0.020-inch-thick mild steel sheet. Figure 5 is a photograph of the small, hand-operated rolling mill used for the operation.

Pack-rolling Operation

The pack was passed through the mill empty until it assumed the slightly curved shape which it retains throughout the rolling operation. A small portion of foil, approximately one inch on a side, was then placed in the sheet steel pack which had been lined with one-mil Mylar film. The

TABLE 3

Results of Reproducibility Investigation of Foil Holder
(Figures quoted are results of fifteen replications;
titanium foils in ports 3, 2, and 1; port 4 vacant;
As K_a radiation used)

Results	Port 4	Port 3	Port 2	Port 1
Mean cps	10,589	4,749.5	4,786.5	4,809.9
Standard deviation	27.696	13.616	14.708	15.621
Coefficient of variation	0.26156	0.28676	0.30736	0.32477

TABLE 4

Semi-Quantitative Spectrographic Analysis of Foils Used in Study

Foil	Impurity					
	Mg	Si	Cu	Cr	Ni	Fe
Titanium	-	-	ND	ND	ND	ND
Vanadium	ND	ND	ND	ND	ND	0.11
Iron	0.002	0.02	0.01	0.1	ND	PC
Nickel	0.002	ND	0.01	0.1	PC	ND
Copper	0.008	0.02	PC	ND	ND	ND
Praseodymium	No impurities could be detected					
Gadolinium						
Erbium						

ND - Not Detected
PC - Principal Constituent

Praseodymium - Chemical Analysis
99.62% Pr

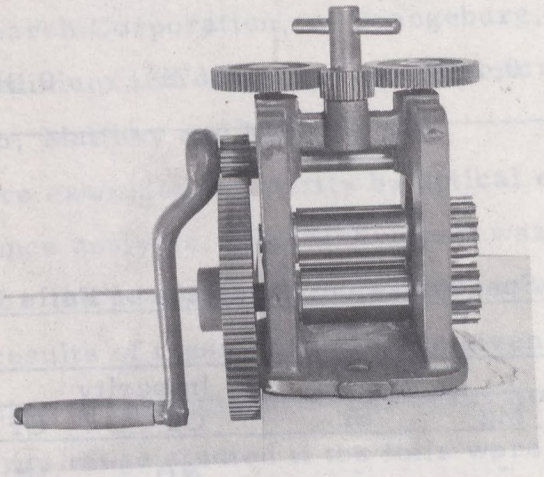

Figure 5. Photograph of hand rolling mill used to pack-roll absorbing foils.

Mylar film was used to prevent metal-to-metal contact. Approximately thirty to forty passes per pack were made; the distance between the rollers was decreased slightly every five passes. The Mylar-coated foil was removed from the pack and clamped under a square brass block, and a razor blade was used to cut an outline of the block around the foil. The Mylar was floated off in carbon tetrachloride, and the foil was rinsed in ethyl ether and weighed. The above process was repeated until a reduction in thickness of forty to fifty per cent had been attained. When this had been accomplished, the foil was rinsed with carbon tetrachloride, benzene and ethyl ether (in that order), weighed two to three times on a Mettler Micro Gram-atic analytical balance, and the area measured with a Gaertner toolmaker's microscope. At least three absorbers of each element were prepared as outlined above.

Assessment of Thickness Uniformity

The assessment of the thickness uniformity of both the pack-rolled and commercial foils was determined by measuring the mass attenuation coefficient in different areas of a foil and comparing the results. This was accomplished by masking the X-ray beam. Two lead masks were used alternately for this purpose, one mask with an aperture in the centre and another mask with the aperture in the first quadrant. Approximately 6 per cent of the foil area was sampled with these masks, as the foil area is approximately 5.5 cm^2 and the aperture area is about 0.33 cm^2. The foils were turned around their centres by 90°, when the mask with the quadrant aperture was in the path, so that different quadrants of the foil could be sampled. Thus, by use of the two masks it was possible to obtain five coefficients, one from each quadrant and one from the centre, in addition to the coefficient for the whole foil. The bulk weight and the area were used to calculate the coefficients. The results of the uniformity measurement are given in Appendix A.

Oxidation of Foils

No special precautions were taken to prevent oxidation of the absorbing foils, except in the case of praseodymium. The transition metals studied are customarily regarded as stable when in a state of high purity and in dry air. The corrosion rates of praseodymium, gadolinium and erbium are listed in Table 5. Since the laboratory in which the measurements were made is maintained at 70°F and 40 per cent relative humidity, it seems reasonable to ignore the corrosion possibilities of gadolinium and erbium. It should be mentioned that the foils were stored in a desiccator under argon and a large flat dish of freshly dried silica gel was placed daily in the spectroscopy chamber of the spectrometer.

A Mylar film was placed over the praseodymium foils to retard oxidation. The foils were pack-rolled for 3 passes, which was sufficient to press firmly together the Mylar film and the praseodymium foil. The film was left on the foil until all the measurements, except weighing, had been completed. Two thicknesses of Mylar were placed in the normally vacant port used to measure the incident intensity, to compensate for the Mylar coating on the foils.

TABLE 5

The Corrosion Rates of Praseodymium, Gadolinium and Erbium in Air*
(Milligrams/Square Decimetre/Day

Temperature (°F)	95		203	
Relative Humidity	< 1%	75%	< 1%	75%
Praseodymium	8	76	900	5,000
Gadolinium	1	2	0	35
Erbium	1	1	0	-

*Ref. 17

X-ray Measurements

The following procedure was used for the X-ray measurements. The power to the X-ray tube was increased until 10,000 cps was obtained for the incident intensity. The detector voltage was set at the midpoint of the counter plateau and the baseline setting was used to eliminate the counter noise. When the gas flow proportional counter was used, the baseline was set to eliminate the argon escape peak, as it has been reported (13) that an increase of 5-10 per cent in the count rate may occur if the count rate due to the escape peak is measured at the same time as the natural peak. The P-10 gas flow rate was very small, of the order of a few litres per hour. The whole spectroscopy chamber of the spectrometer was filled with helium to provide a helium path for measurement of wavelengths greater than 3A. The incident radiation through the vacant port was counted for approximately 36 seconds, collecting 384,000 counts. The foils were moved into the X-ray path and, in most cases, 128,000 counts were collected. The counting times varied from 36 seconds to 300 seconds, depending upon the attenuation of the incident beam. The order of recording the intensities was incident in port 4, foil 3 in port 3, foil 2 in port 2, and foil 1 in port 1. Five replications were made for each sequence. A minimum of three foils was used for each coefficient reported.

Pure elements, whenever available, were used as targets in the sample chamber to produce the K_α and/or K_β wavelengths. Oxides or simple salts, of analytical reagent quality, were used whenever pure elements were not available. A count scan with 0.02-degree 2θ increments was used to obtain the goniometer position for a particular wavelength-analyzing crystal combination.

The intensity measurements were corrected for counting losses by use of the Geiger formula with a dead time of 1.6 microseconds. This dead time was determined by the method of Short (14).

RESULTS

The results of the measurements are given in Tables 6 to 13. The mass attenuation coefficient listed is the arithmetic mean of all the replications. The standard deviation is obtained by taking the square root of the sum of the squares of the deviations from the mean, divided by the degrees of freedom. The coefficient of variation is the standard deviation divided by the arithmetic mean multiplied by 100. Plots of mass attenuation coefficient versus wavelength are given in Figures 6 to 8.

The results were used to calculate values of C and n for the equation:

$$\frac{\mu}{\rho} = C\lambda^n \qquad (4)$$

as proposed by Leroux (5). These values are listed in Table 14. Two sets of values were calculated for all the elements studied because the measurements straddled an absorption edge(s). The mass attenuation coefficients were analyzed for dependence on atomic number by extending Equation 4 to:

$$\frac{\mu}{\rho} = b\,Z^k\,\lambda^n \qquad (5)$$

by a procedure similar to that of Carter et al.(15). Values for the constant b and for the exponents k and n were calculated for the three atomic number-energy regions and are listed in Table 15. The calculation were carried out on a Hewlett-Packard Model 9100A programmable calculator.

TABLE 6

Mass Attenuation Coefficients for Titanium

Wavelength (A)	Mass Attenuation Coefficient (cm^2/gm)	Standard Deviation	Coefficient of Variation
0.9269	50.17	0.3430	0.6837
1.041	68.59	0.2697	0.3932
1.341	138.8	0.7839	0.5648
1.659	248.0	0.8397	0.3386
1.937	376.1	2.968	0.7892
2.103	476.9	3.081	0.6460
2.291	601.5	9.568	1.591
2.504	88.86	0.4748	0.5343
2.748	110.2	0.6714	0.6093
3.359	194.2	0.9450	0.4866
3.742	259.6	0.6182	0.2381
4.728	498.0	4.479	0.8994
5.373	678.9	6.891	1.015

TABLE 7

Mass Attenuation Coefficients for Vanadium

Wavelength (A)	Mass Attenuation Coefficient (cm^2/gm)	Standard Deviation	Coefficient of Variation
0.7107	26.11	0.2098	0.8035
0.9268	55.27	0.1899	0.3436
1.177	107.5	0.4651	0.4327
1.341	153.1	0.4688	0.3062
1.542	221.9	5.154	2.323
1.937	419.7	10.16	2.421
2.103	529.9	8.479	1.600
2.284	74.12	0.2291	0.3091
2.748	123.8	0.4937	0.3988
3.359	227.3	3.926	1.727
3.742	302.5	5.886	1.946
4.728	558.0	5.857	1.050

TABLE 8

Mass Attenuation Coefficients for Iron

Wavelength (A)	Mass Attenuation Coefficient (cm^2/gm)	Standard Deviation	Coefficient of Variation
0.7476	43.10	0.4898	1.136
0.8766	66.83	0.3648	0.5459
1.177	149.7	0.4249	0.2838
1.295	193.5	0.5939	0.3069
1.542	309.9	4.185	1.350
1.659	388.0	5.726	1.476
1.757	53.04	0.1874	0.3533
2.085	86.52	0.2851	0.3295
2.748	189.0	0.5793	0.4065
3.359	334.1	5.053	1.512
3.742	438.0	7.938	1.812

TABLE 9

Mass Attenuation Coefficients for Nickel

Wavelength (A)	Mass Attenuation Coefficient (cm^2/gm)	Standard Deviation	Coefficient of Variation
0.7476	53.55	0.4604	0.8598
0.8766	82.61	0.5269	0.6378
1.106	154.5	1.066	0.6900
1.295	237.0	5.648	2.383
1.436	320.0	4.691	1.466
1.500	44.02	0.3899	0.8857
1.937	89.91	0.5425	0.6034
2.291	144.0	0.7048	0.4894
2.504	185.9	1.00	0.5379
2.748	243.4	5.282	2.170
3.359	419.8	6.516	1.552

TABLE 10

Mass Attenuation Coefficients for Copper

Wavelength (A)	Mass Attenuation Coefficient (cm^2/gm)	Standard Deviation	Coefficient of Variation
0.7476	56.45	0.3642	0.6452
0.8766	87.44	0.5406	0.6183
1.106	163.5	1.120	0.6850
1.341	284.5	2.823	0.9923
1.392	38.22	0.3998	1.046
1.937	97.33	0.6626	0.6808
2.291	156.5	1.352	0.8639
2.504	200.3	1.371	0.6845
2.748	262.7	2.464	0.9380

TABLE 11

Mass Attenuation Coefficients for Praseodymium

Wavelength (A)	Mass Attenuation Coefficient (cm^2/gm)	Standard Deviation	Coefficient of Variation
0.5136	20.72	0.3918	1.891
0.7873	65.71	0.8593	1.308
1.041	138.8	1.865	1.344
1.341	270.4	3.279	1.213
2.085	186.0	1.165	0.6263
2.291	232.3	2.484	1.069
2.504	284.2	3.248	1.143

TABLE 12

Mass Attenuation Coefficients for Gadolinium

Wavelength (A)	Mass Attenuation Coefficient (cm^2/gm)	Standard Deviation	Coefficient of Variation
0.4921	23.68	0.1642	0.6933
0.6147	42.94	0.4284	0.9976
0.7476	72.56	0.4269	0.5883
0.9269	128.2	0.4293	0.3348
1.106	205.3	3.233	1.575
1.255	283.5	4.481	1.580
1.436	394.2	6.285	1.597
1.757	152.6	0.6727	0.4408
2.103	249.2	3.317	1.331
2.291	308.3	4.362	1.415
2.504	363.3	8.918	2.455

TABLE 13

Mass Attenuation Coefficients for Erbium

Wavelength (A)	Mass Attenuation Coefficient (cm^2/gm)	Standard Deviation	Coefficient of Variation
0.4718	25.15	0.1839	0.7322
0.5608	40.10	0.2253	0.5618
0.7107	75.65	0.3062	0.4048
0.8766	130.4	0.6130	0.4701
0.9269	151.4	0.3380	0.2232
1.041	207.8	4.178	2.011
1.128	253.5	5.157	2.034
1.255	325.8	5.788	1.777
1.295	302.2	6.297	2.084
1.341	247.3	4.283	1.732
1.436	291.1	4.409	1.515
1.500	120.3	0.5078	0.4230
1.790	196.4	2.887	1.470
2.291	369.2	5.862	1.588

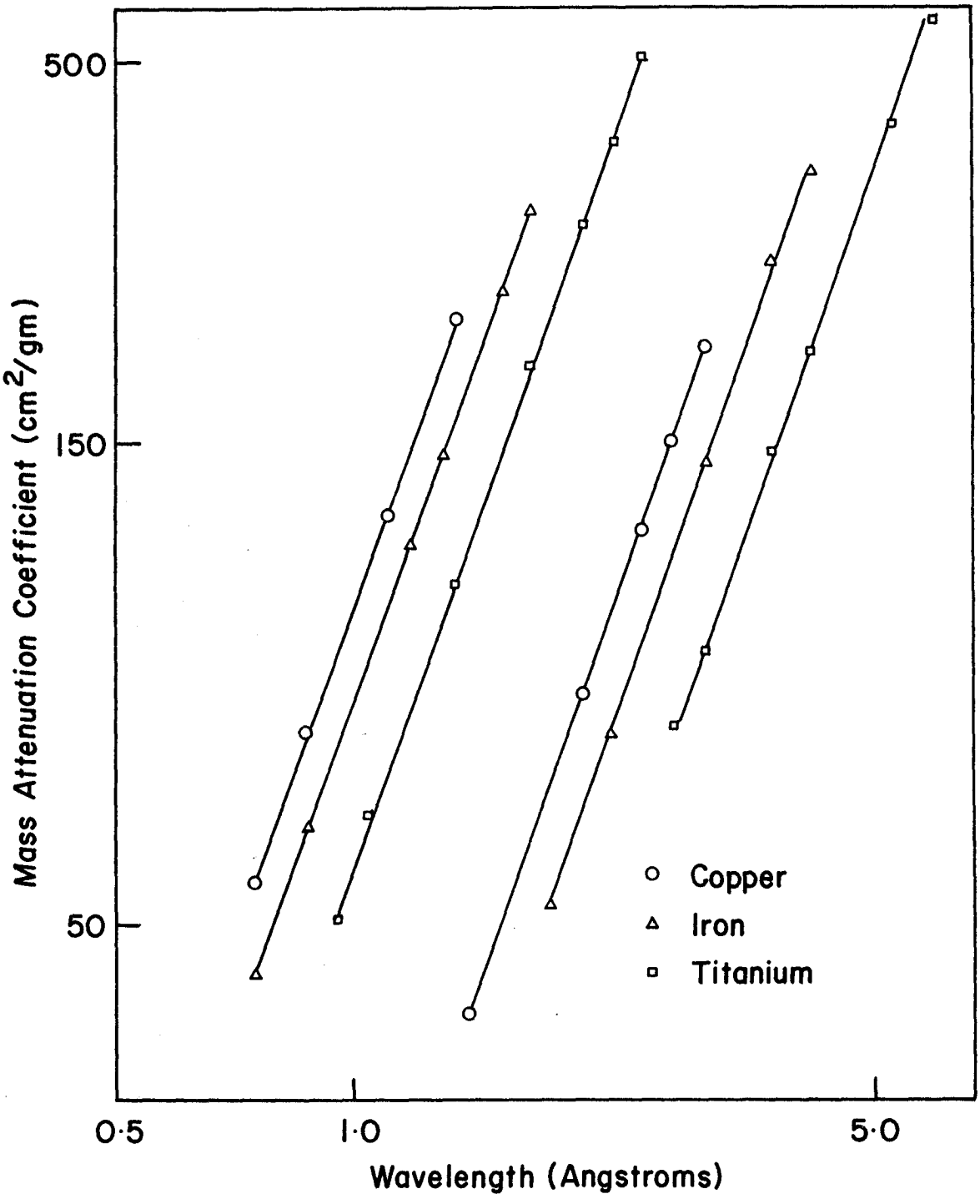

Figure 6 - Plot of mass attenuation coefficient versus wavelength (titanium, iron and copper).

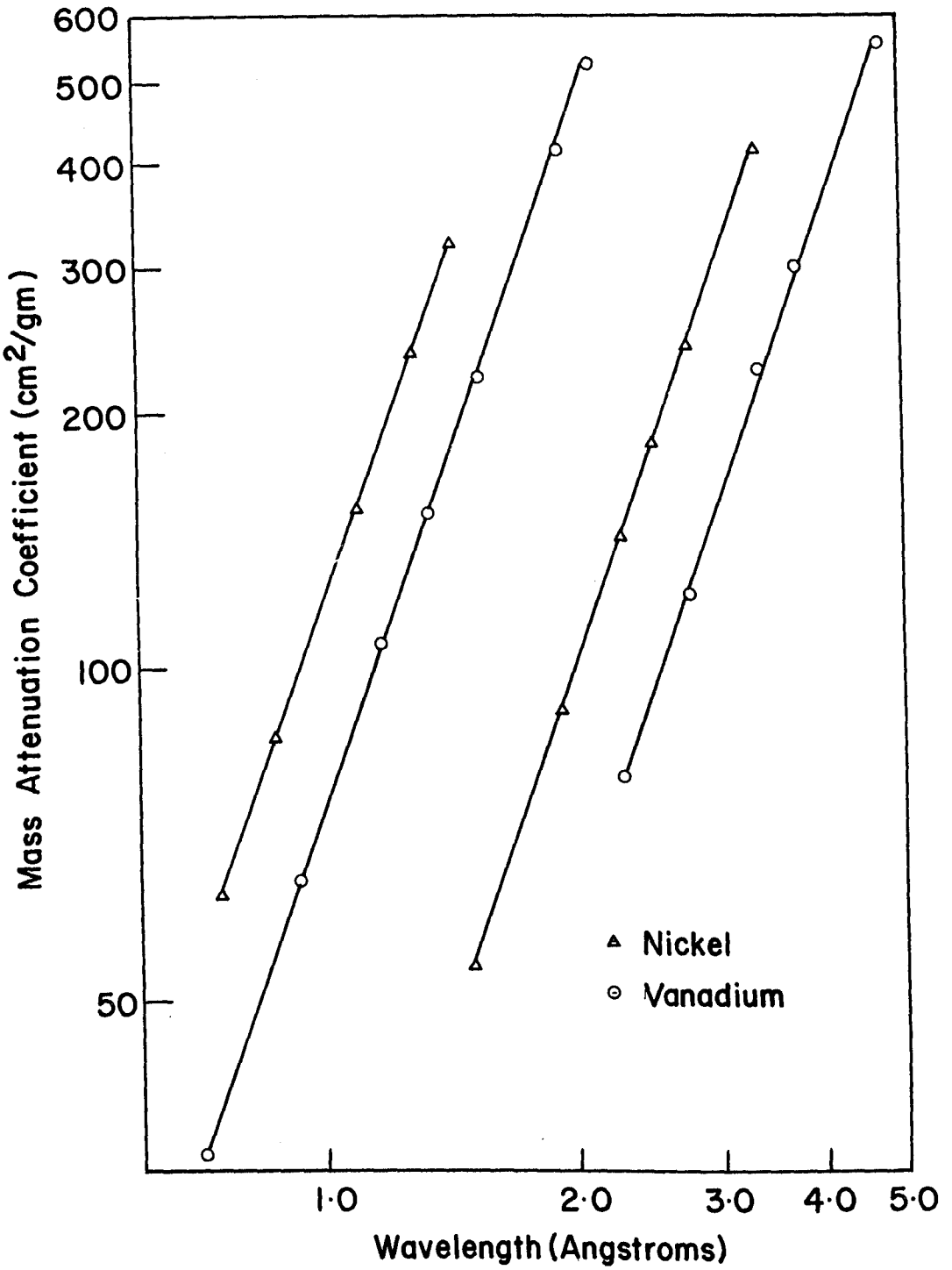

Figure 7 - Plot of mass attenuation coefficient versus wavelength for vanadium and nickel.

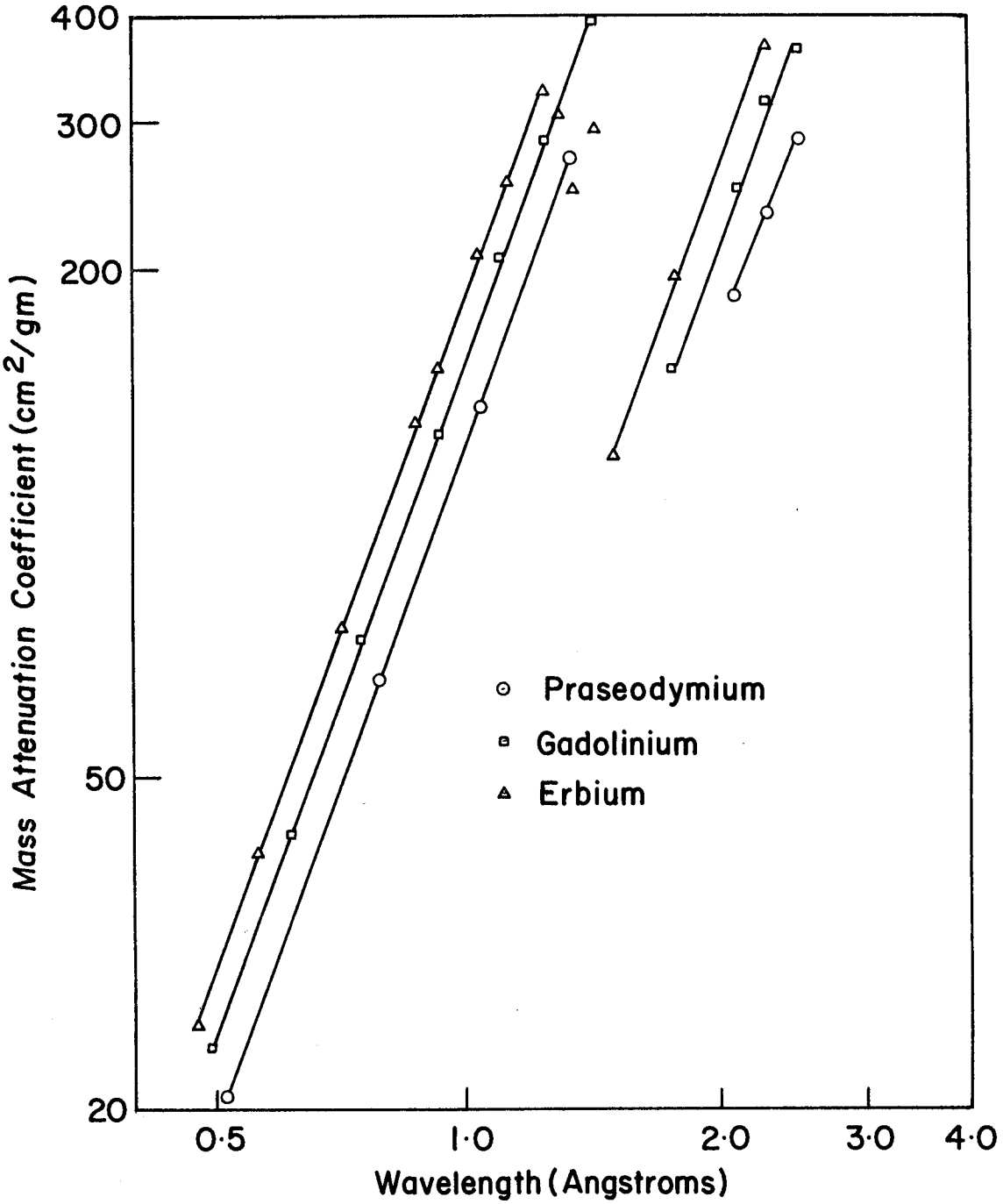

Figure 8 - Plot of mass attenuation coefficient versus wavelength for praseodymium, gadolinium and erbium.

TABLE 14

Values of the Constant C and the Exponent n for the Expression $\frac{\mu}{\rho} = C\lambda^n$ Calculated from the Experimental Data

Element	Z	$\lambda < \lambda_{k_A}$		$\lambda_{k_A} < \lambda < \lambda_{LI_A}$		$\lambda_{LIII_A} < \lambda < \lambda_{MI_A}$	
		C	n	C	n	C	n
Titanium	22	61.71	2.746	7.382	2.696	-	-
Vanadium	23	67.84	2.760	7.566	2.782	-	-
Iron	26	95.91	2.736	11.14	2.794	-	-
Nickel	28	118.2	2.718	14.13	2.804	-	-
Copper	29	125.9	2.747	15.00	2.829	-	-
Praseodymium	59	-	-	124.0	2.678	33.97	1.531
Gadolinium	64	-	-	155.1	2.632	38.38	2.481
Erbium	68	-	-	183.7	2.626	41.81	2.640

λ_{kA} - Wavelength of the K absorption edge.

λ_{LIA} - Wavelength of the L_I absorption edge.

$\lambda_{L_{IIIA}}$ - Wavelength of the L_{III} absorption edge.

λ_{MIA} - Wavelength of the M_I absorption edge.

TABLE 15

Values of the Constant and the Exponents for the Expression

$\frac{\mu}{\rho} = bZ^k\lambda^n$ Calculated from the Experimental Data

Z, λ Region	b	k	n
z = 22 to 29 $\lambda < \lambda_{kA}$	0.01603	2.668	2.750
z = 22 to 29 $\lambda_{kA} < \lambda < \lambda_{LIA}$	0.0003746	3.163	2.784
z = 59 to 68 $\lambda_{kA} < \lambda < \lambda_{LIA}$	0.001216	2.827	2.644

λ_{kA} - Wavelength of the K absorption edge.

λ_{LIA} - Wavelength of the L_I absorption edge.

DISCUSSION

Perhaps the most complete way of assessing the uncertainty in an experiment where the item of interest is given by some function from directly measurable quantities, is by the application of the law of propagation of error (16). If $Z = f(x_1, x_2, \text{"'})$ is some function of random quantities, the variance S_z^2 may be approximated by the expression

$$S_z^2 \simeq \left(\frac{f}{x_1}\right)^2 S_{x_1}^2 + \left(\frac{f}{x_2}\right)^2 S_{x_2}^2 + \text{"'} \qquad (6)$$

Heinrich has used this law to obtain an expression, similar to Equation 7 below, for the standard deviation of an absorption coefficient considering only random errors.

$$S_{\frac{\mu}{\rho}} = \left[(\ln P)^2 \left(\frac{S_A^2}{w^2} + \frac{A^2}{w^2} \left[\frac{1}{N_o} + \frac{1}{N} \right] \right) \right]^{-1/2} \qquad (7)$$

The derivation of this expression and an explanation of its terms are given in Appendix B. By the use of this equation, it is possible to show that a coefficient of variation of less than one per cent may be obtained over a considerable transmission range. The data used for these calculation are presented in Table 16.

The non-uniformity in thickness of an absorbing foil is, however, the major error in the determination of an attenuation coefficient, but this error is not included in Equation 7. The fractional shift in transmission, $\Delta T/T$, where T is defined as the ratio of attenuated to incident intensity, due to a fractional change in thickness x, is given by :

$$\frac{\Delta T}{T} = \mu \Delta x \qquad (8)$$

where μ is the linear attenuation coefficient. The derivation of this expression is given in Appendix C.

TABLE 16

Data Used to Calculate the Coefficient of Variation of the Mass Attenuation Coefficient as Predicted by the Law of Propagation of Error

N_o	N	t_o	t	τ	$S^2_{\frac{\mu}{\rho}}$	$\frac{\mu}{\rho}$	c.v.
384,000	384,000	36	45	0.80	0.14	34.8	1.06
			60	0.60	0.17	79.7	0.52
			75	0.48	0.22	114.5	0.41
	192,000		45	0.40	0.34	142.9	0.41
			60	0.30	0.45	187.8	0.36
			75	0.24	0.55	222.6	0.33
	96,000		45	0.22	0.74	239.2	0.36
			60	0.16	0.91	284.1	0.32
			75	0.13	1.07	318.9	0.32
			120	0.080	1.45	392.2	0.31
			215	0.045	2.03	483.1	0.30
	64,000		300	0.02	3.75	610.2	0.32
			600	0.01	8.23	718.3	0.40

N_o - Number of counts collected for incident intensity.

N - Number of counts collected for attenuated intensity.

t_o - Time taken to collect incident intensity.

t - Time taken to collect attenuated intensity.

τ - The ratio of attenuated to incident intensities.

$S^2_{\frac{\mu}{\rho}}$ - The variance of the mass attenuation coefficient as predicted by Equation 7.

$\frac{\mu}{\rho}$ - The mass attenuation coefficient using the weight and area data for rolled iron foil #2.

c.v. - Coefficient of variation, $S_{\frac{\mu}{\rho}}$ divided by $\frac{\mu}{\rho}$.

A simple calculation will show that a two per cent fractional change in thickness will result in a two per-cent uncertainty in the attenuation coefficient. Expressions developed by Carter et al.(15) and Halliday et al. (12) confirm that non-uniformity in thickness introduces a large error.

The calculated sample standard deviation, that is, the square root of the sums of the squares of the deviations from the mean, is in sporadic agreement with that predicted by Equation 7. However, Equation 7 does not take cognizance of non-random errors and, without doubt, the large discrepancies between measured and predicted standard deviations can be attributed to non-uniformity in the thickness of the foils.

Heinrich's tables (2) of mass attenuation coefficients are regarded as the most reliable to date; hence a comparison is made between the results of this study and his tables in Table 17. Agreement between the two for titanium is good. For vanadium, Heinrich's coefficients are consistently higher by a small amount, somewhat less than two per cent in most cases. The vanadium coefficients determined by Carter et al.(15) are also slightly less than those of Heinrich, substantiating the results of this study. The agreement with iron is good except for the coefficient at $\lambda = 3.359$, where the disagreement is of the order of four per cent. Carter's studies also indicate that Heinrich is slightly low in this energy range for iron. There is consistent disagreement for nickel: nine of the eleven measured coefficients are higher than Heinrich's by one to two per cent. The work of Hughes et al.(4) also supports these observations. The agreement with copper is good, except in the region just beyond the K absorption edge where there is a discrepancy of two per cent.

Comparison between Heinrich's tables and the measured coefficients for the rare earth is somewhat different than for the transition elements, insofar as very little, if any, published data were available to Heinrich as a basis for his calculations. If the measurements for this study are used as a reference point, then Heinrich's calculations for the rare earths are remarkably accurate. There are some areas of disagreement, especially around the L_I absorption edge of erbium, and for gadolinium from 1.5A to 2.5A, but in general agreement is good.

TABLE 17

Comparison of Measured Mass Attenuation Coefficients With Those from Heinrich's Tables

Element	Wavelength (Å)	Measured Coefficient	Heinrich's Tables
Titanium	0.9269	50.17	50.5
	1.041	68.59	69.3
	1.341	138.8	138.3
	1.659	248.0	247.3
	1.937	376.1	377.5
	2.103	476.9	472.5
	2.291	601.5	597.0
	2.504	88.86	85.8
	2.748	110.2	110.6
	3.359	194.2	191.3
	3.742	259.6	256.8
	4.728	498.0	486.4
	5.373	678.9	689.6
Vanadium	0.7107	26.11	27.4
	0.9269	55.27	56.8
	1.177	107.5	108.9
	1.341	153.1	155.5
	1.542	221.9	227.7
	1.937	419.7	424.3
	2.103	529.9	531.1
	2.284	74.12	76.5
	2.748	123.8	126.7
	3.359	227.3	219.1
	3.742	302.5	294.3
	4.728	558.0	557.2
Iron	0.7476	43.10	43.2
	0.8766	66.83	66.8
	1.177	149.7	149.2
	1.295	193.5	193.5
	1.542	309.9	311.1
	1.659	388.0	379.6
	1.757	53.04	54.7
	2.085	86.52	87.3
	2.748	189.0	185.6
	3.359	334.2	321.1
	3.742	438.0	431.1

- Concluded

TABLE 17 (Concluded)

Element	Wavelength (Å)	Measured Coefficient	Heinrich's Tables
Nickel	0.7476	53.55	52.4
	0.8766	82.61	81.0
	1.106	154.5	152.3
	1.295	237.0	233.5
	1.436	320.0	309.0
	1.500	44.02	44.8
	1.937	89.91	90.0
	2.291	144.0	142.3
	2.504	185.9	181.4
	2.748	243.4	233.8
	3.359	419.8	404.4
Copper	0.7476	56.45	57.3
	0.8766	87.44	88.6
	1.106	163.5	166.6
	1.341	284.5	280.8
	1.392	38.22	40.6
	1.937	97.33	100.0
	2.291	156.5	158.1
	2.504	200.3	201.6
	2.748	262.7	259.8
Praseodymium	1.041	138.8	139.8
	1.341	270.4	275.5
	2.085	186.0	178.8
	2.291	232.3	228.5
	2.504	284.2	287.9
Gadolinium	0.9269	128.2	128.3
	1.106	205.3	205.3
	1.255	283.5	287.3
	1.436	394.2	411.1
	1.757	152.6	148.5
	2.103	249.2	237.0
	2.291	308.3	296.1
	2.504	363.3	373.1
Erbium	0.8766	130.4	129.7
	0.9269	151.4	150.6
	1.041	207.8	204.6
	1.128	253.5	252.9
	1.255	325.8	335.1
	1.295	302.2	310.7
	1.341	247.3	245.2
	1.436	291.1	293.7
	1.500	120.3	119.6
	1.790	196.4	189.4
	2.291	369.2	459.8

The values calculated for the constant and the exponent in the expression $\mu/\rho = C\lambda^n$ are not in good agreement with those calculated by Heinrich. The discrepancies approach ten per cent in some cases. In the region between the K and L absorption edges for the transition elements. Heinrich lists a value for the exponent of 2.73, while the values for this study increase steadily with atomic number from 2.70 to 2.83.

There is a slight discrepancy in the exponent n for the rare earths in the region between the K and L absorption edges. The exponent from this study is consistently larger by about one per cent than that of Heinrich. There is a discrepancy, of the order of twenty per cent, in the region beyond the L absorption edge in the case of the constant for pradeodymium and gadolinium, but, surprisingly, not for erbium.

There is no readily available source to compare the values for the constant and exponents calculated for the expression $\mu/\rho = b Z^k \lambda^n$. Carter et al.(15) calculated values for the constant and exponents for this expression but did so for all elements over the entire energy range studied, apparently taking no cognizance of absorption edges.

ACKNOWLEDGEMENTS

The author would like to express his gratitude to Dr. A.H. Gillieson whose sustained interest and encouragement made this project possible. I would like to extend thanks to Mrs. D. Reed for many helpful discussions concerning the project, to Mr. P. Weber Hall for construction of the device to insert the absorbers into the X-ray path, and to Mr. J. Krzyzewski who designed and constructed the control circuits for the device. Thanks are also due to Mr. G.L. Mason and Mr. D. Norman for assistance in the pack-rolling aspect of the project. Dr. H.P. Dibbs contributed to the project with a helpful discussion on the assessment of error.

REFERENCES

1. Heinrich, Kurt F.J., Technical Note 284, National Bureau of Standards, Washington, D.C. (1966).
2. Heinrich, Kurt F.J., "The Electron Microprobe" (edited by McKinley, Heinrich and Wittry), John Wiley and Sons, New York, p. 296 (1966).
3. Stainer, H.M., U.S. Bureau of Mines Circular 8166 (1963).
4. Hughes, G.D., Woodhouse, J.B. and Bucklow, I.A., Brit. J. Appl. Phys. Ser. 2, Vol. 1, p. 695 (1968).
5. Leroux, J., Advances in X-ray Analysis, 5, 153 (1961).
6. Kelly, T.K., Trans., Inst. Min. Met. (London), 75, B 59 (1966).
7. Compton, A.H. and Allison, S.K., "X-rays in Theory and Experiment", MacMillan and Co. Ltd., London, p. 799 (1935).
8. Evans, R.D., Encyclopedia of Physics, XXXIV, Springer-Verlag, Berlin, p. 219 (1958).
9. Klein, O. and Nishina, Y., Z. Physik, 52, 853 (1929).
10. Grodstein, G. White, National Bureau of Standards Circular 583 (1957).
11. Hubbell, J.H., National Bureau of Standards report NSRDS-NBS-29 (August 1969), 85 pp.
12. Halliday, F.O., Keast, A.K., Kelman, J.F. and Passel, T.O., J. Appl. Phys., 38, No. 4, 1874 (1967).
13. Jenkins, R. and de Vries, J.L., "Practical X-ray Spectrometry", Philips Technical Library, Springer-Verlag, New York (1968).
14. Short, M.A., Rev. Sci. Instr., 31, 618 (1960).
15. Carter, R.W., Rohrer, R.H., Carlton, W.H. and Dyer, G.R., Health Physics, 13, 593 (1967).
16. Nalimov, V.V., "The Application of Mathematical Statistics to Chemical Analysis", Addison-Wesley Publishing Co., Reading, Mass., p. 34 (1963).
17. Rare Metals Handbook, Reinhold Publishing Co., London (1961).

=====

JLD:(PES)PG

APPENDIX A

Results of Uniformity Investigation of Purchased and Pack-Rolled Absorbing Foils

Foil	Predicted Coefficient	Measured Coefficients for Different Areas					
		Whole Foil	Centre	Quadrants			
				1st	2nd	3rd	4th
Ti 3	96.9	97.42	97.07	96.99	96.95	-	-
Ti 2		97.05	96.65	97.06	96.63	-	-
Ti 1		97.50	96.68	97.09	96.75	-	-
Ti 4R	247.3	243.8		246.5	-	241.5	-
Ti 3R		247.5	247.3	246.9	247.2	-	-
Ti 2R		251.5	258.2	262.8	252.0	-	-
Ti 1R		250.4	256.1	249.7	-	-	255.8
V 3	77.9	75.06	75.14	74.44	75.32	-	-
V 2		75.29	75.19	75.53	75.35	-	-
V 1		75.39	75.55	75.83	75.33	-	-
V 4R	278.0	282.2	279.4	285.9	-	277.9	-
V 2R		274.0	272.5	274.0	280.5	-	-
V 3R	227.7	225.0	223.4	237.4	213.4	-	-
V 1R		232.0	221.2	235.3	-	-	228.1
Fe 1	78.0	76.60	77.18	77.21	76.86	76.52	77.10
Fe 3R	177.7	177.4	179.1	174.7	181.2	179.0	174.3
Fe 2R		179.1	181.0	180.4	180.6	181.0	172.9
Fe 1R		180.9	179.8	179.8	179.4	179.2	187.2
Ni 1	94.4	96.11	95.67	96.47	96.5	97.42	96.51

Concluded on next page -

APPENDIX A(Concluded)

Foil	Predicted Coefficient	Measured Coefficients for Different Areas					
		Whole Foil	Centre	Quadrants			
				1st	2nd	3rd	4th
Ni 5R	214.5	222.1	218.9	226.4	-	213.5	-
Ni 4R		215.2	211.2	217.0	223.8	-	-
Ni 3R	180.3	184.9	186.2	189.0	189.2	186.1	184.6
		179.7	179.2	181.3	187.7	173.6	175.0
Cu 1	103.3	100.5	100.4	99.40	100.1	100.3	99.81
Cu 3R	123.4	124.1	121.7	126.6	122.2	123.4	127.5
Cu 2R		121.7	123.3	124.1	125.1	122.3	120.0
Cu 1R		122.6	124.7	122.3	112.0	123.1	121.9
Gd 3	-	61.88	62.41	59.74	61.36	-	-
Gd 2		61.94	62.44	61.63	62.47	-	-
Gd 1		63.31	62.58	63.41	62.84	-	-
Gd 3R	128.3	127.9	127.9	127.7	131.0	-	-
Gd 2R		126.5	126.2	129.1	125.1	-	-
Gd 1R		126.9	125.5	127.8	128.5	-	-
Er 3	-	50.07	50.06	50.70	50.17	-	-
Er 2		49.96	50.24	50.85	50.36	-	-
Er 1		51.10	50.49	50.56	50.50	-	-
Er 6R	150.6	154.1	155.9	147.9	149.5	-	-
Er 5R		151.3	150.9	152.2	155.2	-	-
Er 4R		148.4	148.9	153.9	157.1	-	-
Er 3R		155.1	155.2	150.1	151.4	-	-
Er 2R		149.3	150.3	153.3	155.3	-	-
Er 1R		154.9	156.8	154.5	151.2	-	-

R - denotes a pack-rolled foil.
Predicted Coefficient taken from Heinrich's tables.

APPENDIX B

Derivation of Expression for Standard Deviation of Mass Attenuation Coefficient Using the Law of Propagation of Error

Apply Equation 3:

$$I = I_o \exp\left(-\frac{\mu}{\rho}\rho x\right) \qquad (B.1)$$

Rearranging:

$$\frac{\mu}{\rho} = \frac{1}{\rho x} \ln \frac{I_o}{I} \qquad (B.2)$$

$$\rho x = \frac{w}{A} \quad , \qquad (B.3)$$

where w and A are the weight and area of the foil respectively.

Apply law of propagation of error:

$$S^2_{\frac{\mu}{\rho}} = \left(\frac{\partial \frac{\mu}{\rho}}{\partial A}\right)^2 S^2_A + \left(\frac{\partial \frac{\mu}{\rho}}{\partial w}\right)^2 S^2_w \left(\frac{\partial \frac{\mu}{\rho}}{\partial \frac{I_o}{I}}\right)^2 S^2_{\frac{I_o}{I}} \qquad (B.4)$$

$$\left(\frac{\partial \frac{\mu}{\rho}}{\partial A}\right) = \frac{1}{w} \ln \frac{I_o}{I}$$

$$\left(\frac{\partial \frac{\mu}{\rho}}{\partial w}\right) = -\frac{A}{w^2} \ln \frac{I_o}{I} \qquad (B.5)$$

$$\left(\frac{\partial \frac{\mu}{\rho}}{\partial \frac{I_o}{I}}\right) = \frac{A}{w} \frac{1}{\frac{I_o}{I}}$$

$$\text{Set } P = \frac{I_o}{I} \qquad (B.6)$$

$$S^2_{\frac{\mu}{\rho}} = \left(\frac{\ln P}{w}\right)^2 S^2_A + \left(\frac{-A}{w^2}\ \ln P\right)^2 S^2_w + \left(\frac{A}{w}\ \frac{1}{p}\right)^2 S^2_p \qquad (B.7)$$

A microgram analytical balance was used to weigh the foils; therefore S^2_w is very small and may be deleted.

$$S^2_{\frac{\mu}{\rho}} = \left(\frac{\ln P}{w}\right)^2 S^2_A + \left(\frac{A}{w}\ \frac{1}{p}\right)^2 S^2_p \qquad (B.8)$$

$$P = \frac{I_o}{I} = \frac{N_o}{N}\ \frac{t}{t_o}\ , \qquad (B.9)$$

where N_o and N are the number of counts collected for the incident and attenuated intensity in times t_o and t, respectively. Apply propagation of error to (B.9):

$$S^2_p = \left(\partial \frac{P}{N_o} \Big/ \partial \frac{}{N}\right)^2 S^2_{\frac{N_o}{N}} + \left(\partial \frac{P}{\frac{t}{t_o}}\right)^2 S^2_{\frac{t}{t_o}} \qquad (B.10)$$

$S^2_{\frac{t}{t_o}}$ is small and may be deleted.

$$S^2_p = \left(\partial \frac{P}{N_o} \Big/ \partial \frac{}{N}\right)^2 S^2_{\frac{N_o}{N}} \qquad (B.11)$$

$$\partial \frac{P}{N_o} \Big/ \partial \frac{}{N} = \frac{t}{t_o}$$

$$S^2_{\frac{N_o}{N}} = \left(\partial \frac{N_o}{N} \Big/ \partial N_o\right)^2 S^2_{N_o} + \left(\partial \frac{N_o}{N} \Big/ \partial N\right)^2 S^2_N \qquad (B.12)$$

$$S^2\frac{N_o}{N} = S^2_{\frac{N_o}{N}} + \frac{N_o^2}{N^4} S^2_N \qquad (B.13)$$

According to counting statistics:

$$S^2 N_o = N_o \qquad S^2 N = N$$

$$S^2_{\frac{N_o}{N}} = \frac{N_o}{N^2} + \frac{N_o^2}{N^3} \qquad (B.14)$$

Introduce (B. 14) into (B. 11).

$$S^2 p = \left(\frac{t}{t_o}\right)^2 \left(\frac{N_o}{N}\right)^2 \left[\frac{1}{N_o} + \frac{1}{N}\right] \qquad (B.15)$$

Introduce (B. 15) into (B. 8).

$$S^2 \frac{\mu}{\rho} = \left(\frac{\ln P}{w}\right)^2 S^2_A + \left(\frac{A}{w} \cdot \frac{1}{P}\right)^2 \left(\frac{1}{t_o}\right)^2 \left(\frac{N_o}{N}\right)^2 \left[\frac{1}{N_o} + \frac{1}{N}\right] \qquad (B.16)$$

Cancelling in the second term:

$$S^2 \frac{\mu}{\rho} = \left(\frac{\ln P}{w}\right)^2 S^2_A + \left(\frac{A}{w}\right)^2 \left[\frac{1}{N_o} + \frac{1}{N}\right] \qquad (B.17)$$

—

APPENDIX C

Derivation of Expression for the Fractional Shift in Transmission Due to Non-Uniformity of Absorber

Apply Equation 2:

$$\frac{I}{I_o} = T_x = \exp^{(-\mu x)} \qquad (C.1)$$

Introduce an increment x to thickness x:

$$\frac{I}{I_o} = T_{x+\Delta x} = \exp^{-\mu (x+\Delta x)} \qquad (C.2)$$

Subtract (C.2) from (C.1):

$$T_x - T_{x+\Delta x} = \exp(-\mu x) - \exp(-\mu x - \mu \Delta x) \qquad (C.3)$$

$$\Delta T = \exp(-\mu x)\left[1 - \exp(-\mu \Delta x)\right] \qquad (C.4)$$

$$T = \exp(-\mu x) \qquad (C.5)$$

$$\frac{\Delta T}{T} = 1 - \exp(-\mu \Delta x) \qquad (C.6)$$

Apply exponential series:

$$e^x = 1 + x + \frac{x^2}{2!} \qquad (C.7)$$

Ignore all terms beyond first order and substitute into (C.6).

$$\frac{\Delta T}{T} = 1 - (1 - \mu \Delta x) \qquad (C.8)$$

$$\frac{\Delta T}{T} = \mu \Delta x \qquad (C.9)$$